Modified Steel-Jacketed Columns for Combined Blast and Seismic Retrofit of Existing Bridge Columns

Pierre Fouché[1]; Michel Bruneau, F.ASCE[2]; and Vincent P. Chiarito, M.ASCE[3]

Abstract: Steel jacketing has been used extensively in the United States to retrofit seismically deficient bridge columns. This procedure, which consists of encasing a RC column in a steel jacket, is effective in providing a ductile seismic response but does not enhance the blast resistance of the column. This is because a gap is typically left at the top and bottom of the jacket to prevent increased flexural strength, such as to avoid undesirable overload of the footing or cap beam. Blast tests have demonstrated that direct shear failure can develop at these gap locations. A modification to steel-jacketed columns is proposed here to provide an added blast resistance. It consists of structural steel collars placed around the gaps and tied to the adjacent elements with postinstalled anchors. Blast tests were conducted to investigate the effectiveness of this simple proposed detail. Experimental results indicated that the concept was effective in preventing direct shear failure. Severe blast load demands were applied to investigate the behavior of the retrofitted column under extreme ductility demands. All specimens exhibited satisfactory ductile behavior, except one, which uncharacteristically failed due to fracture of the tube's vertical weld seam. **DOI: 10.1061/(ASCE)BE.1943-5592.0000882.** © *2016 American Society of Civil Engineers.*

Author keywords: Jacketed column; Retrofit; Blast testing; Inelastic response; Direct shear; Plastic hinging.

Introduction

In many parts of the United States, particularly in California, reinforcement detailing requirements in effect decades ago resulted in RC bridge columns that exhibited nonductile behavior during earthquakes (Housner and Thiel 1990). Many methods have been used to retrofit such nonductile columns (Priestley et al. 1996). One of the most popular methods, steel jacketing, has been commonly used across the United States (Priestley et al. 1994; Chai 1996; Shams and Saadeghvaziri 1997; Kim and Shinozuka 2004). A steel-jacketed column (SJC) is created by adding a steel shell that provides confinement to the concrete. This steel jacket allows plastic hinges to develop at the top and bottom of the column, where plastic hinges would be unable to form in a nonductile column without adequate transverse reinforcement.

A column retrofitted with a steel jacket may visually resemble a concrete-filled steel tube composite column, but it does not behave similarly because the jacket is typically discontinuous at the column top and base to avoid undesirable overload of the adjacent members (i.e., footing or cap beam) due to composite action that would significantly increase the flexural strength of the column (Buckle et al. 2006). As a result, although wrapping a concrete column with a steel jacket is widely accepted as a cost-effective retrofit technique for columns of seismically deficient bridges, the merits of this technique do not translate into improved blast performance for bridge columns. In tests performed by Fujikura et al. (2008) and Fujikura and Bruneau (2011), direct shear failure under blast load was observed at the gaps between the jacket and the surrounding footing when exposed to blast, and analyses have supported this observation (Fujikura and Bruneau 2012).

To prevent this undesirable failure mode without hindering the initial role of the jacket, the use of structural steel collars placed around the gaps and tied to the adjacent elements with postinstalled anchors as a technique to increase shear strength locally was proposed. A nonstick interface material inserted between the collar and the column allows smooth contact, thus increasing only shear strength while leaving flexural strength of the column virtually unchanged (as intended by the initial jacketing design). This concept is referred to here as a modified SJC (MSJC). This paper documents the results of blast tests conducted to investigate the effectiveness of this proposed MSJC system (Fouché and Bruneau 2014). Furthermore, because it is customary in blast engineering papers not to report charge weights and standoff distances, shorting pins were used to calculate specimen velocity to provide data that can be used by the broader research community in future analytical work. The resulting impulses calculated from those measured velocities are presented in the last section of this paper.

Specimen Design and Experimental Setups

Specimens were quarter scale of prototype columns in multicolumn bridge pier bents, part of a typical three-span continuous highway bridge (prototype span lengths of 35, 25, and 30 m). Note that scale testing has gained substantial acceptance in blast engineering over the past decade and was proven to provide reliable results and key knowledge in understanding the behavior of structures subjected to blast (Woodson and Baylot 1999; Williams et al. 2008; J. Ray, personal communication, 2008). The work conducted here was performed with the same mindset. Future research at larger scales for

[1]Consultant, Haiti; formerly, Graduate Research Assistant, Dept. of Civil, Structural, and Environmental Engineering, Univ. at Buffalo, Buffalo, NY 14260.

[2]Professor, Dept. of Civil, Structural, and Environmental Engineering, Univ. at Buffalo, Buffalo, NY 14260 (corresponding author). E-mail: bruneau@buffalo.edu

[3]Research Structural Engineer, CEERD-GSS, 3909 Halls Ferry Rd., U.S. Army Engineer Research and Development Center, Vicksburg, MS 39180-6199.

Note. This manuscript was submitted on June 1, 2015; approved on October 21, 2015; published online on February 11, 2016. Discussion period open until July 11, 2016; separate discussions must be submitted for individual papers. This paper is part of the ***Journal of Bridge Engineering***, © ASCE, ISSN 1084-0702.

the same scaled distance could further validate the findings presented here.

For consistency in comparing results, the jacketed columns (prior to adding the blast retrofit collars) were designed and built to be identical to those used in prior blast tests in which direct shear failure was observed (Fujikura and Bruneau 2011). Specimens consisted of nonductile RC columns retrofitted by adding a steel shell that provides confinement to the concrete and allows plastic hinges to develop at the top and bottom of the column.

The 1,500-mm (65-in.) tall nonductile RC column specimens all had a diameter of 200 mm (8 in.). D3 deformed steel wires served as flexural reinforcement, and D1 wires served as spiral (shear) reinforcement. The average diameter of a D3 wire is 4.95 mm (0.195 in.), and its average area is 19.35 mm^2 (0.03 $in.^2$); those of a D1 wire are 2.87 mm (0.113 in.) and 6.45 mm^2 (0.01 $in.^2$), respectively. The mechanical properties of deformed wires are different from those of rebar; thus, they were annealed to confer to them properties similar to those of rebar. During the annealing process, the wires were placed in a vacuum furnace and heated to 1,135°F for 12 h overnight for two nights, consecutively. The resulting average stress–strain curve obtained for the wires after this process is shown in Fig. 1(a).

The nonductile RC columns were then retrofitted using a steel jacket designed in accordance with the procedure developed by Chai et al. (1991) and as reported by Buckle et al. (2006). The steel plate used for the jacket was a cold-rolled commercial steel sheet complying with ASTM 1008 CS (ASTM 2015). Typically, this steel has a yield strength of between 140 and 280 MPa (20 and 40 ksi) and an elongation at failure of 30% minimum of 50 mm (2 in.). For the quarter-scale model of this experimental series, the thickness of the steel jacket was specified to be 1.2 mm (18-gauge plate with a thickness of 0.048 in.). The corresponding stress–strain curve obtained for a coupon of this material is given in Fig. 1(b). To create the required gap of 13 mm (0.5 in.) at the top and bottom of the RC SJC (as specified by Caltrans 1996), 13-mm (0.5-in.) thick plywood pieces with a 203-mm (8-in.) diameter hole were inserted between the steel jacket and the footing and cap beam. Self-consolidating concrete with a strength of 35 MPa (5 ksi) was cast in place to form the core. Concrete with a minimum expected strength of 28 MPa (4 ksi) was used to cast the cap beam. As a result, the specimens (prior to the proposed enhanced collar retrofit) were identical to the previously tested specimens that had failed in direct shear (Fujikura et al. 2008; Fujikura and Bruneau 2011).

The structural steel collars placed around the gaps at the top and bottom of the jacketed columns to help increase the shear strength locally were made by welding two halves of an A53 steel tube 216 mm (8.5 in.) in diameter with a thickness of 8 mm (0.3125 in.) to a 9.5-mm A36 steel plate (the two halves of the A53 tubes were welded together at the seams). This assembly was then tied to the adjacent elements (cap beam and footing) with concrete anchors 19.05 mm (0.75 in.) in diameter. A nonstick interface between the collar and the column was created using Rulon tape (Saint-Gobain, Hoosick Falls, New York) to allow only smooth contact between the collar and the jacketed column, thus increasing only shear strength while leaving the flexural strength of the column virtually unchanged, as normally intended in steel jacketing. The collar components before and after assembly are shown in Fig. 2.

The experimental setup used for this test series was also similar to the one used for the prior tests. In all cases, the bents were laterally supported by a reaction frame, which also served to simulate the boundary condition and rigidity at the top of the bent beam that the deck of a full-scale bridge would have provided.

In all cases, the assumed blast scenario initially considered was the detonation of explosives located inside a small vehicle below the bridge deck at a close distance to the column, but the intensity of blast forces was eventually increased beyond this scenario to push the columns to greater inelastic deformations.

Design of MSJC Base Retrofit

For design of the base retrofit of the MSJC, it was assumed that the collar and the SJC were fully decoupled. In that case, the SJC would resist moment at the base of the specimen, and the collar would supply the shear strength needed to prevent direct shear failure. The thickness of the collar was thus calculated assuming that the shear associated with the flexural capacity of the SJC was to be resisted by the effective area in shear of the collar, such that

$$f_{vc} = \frac{2V_{pr}}{A_{c\_\text{eff}}} \tag{1}$$

where an arbitrary safety factor of 2 was used; and f_{vc} is the shear strength of the collar, taken as $0.6F_{yc}$ (with F_{yc} being the yield

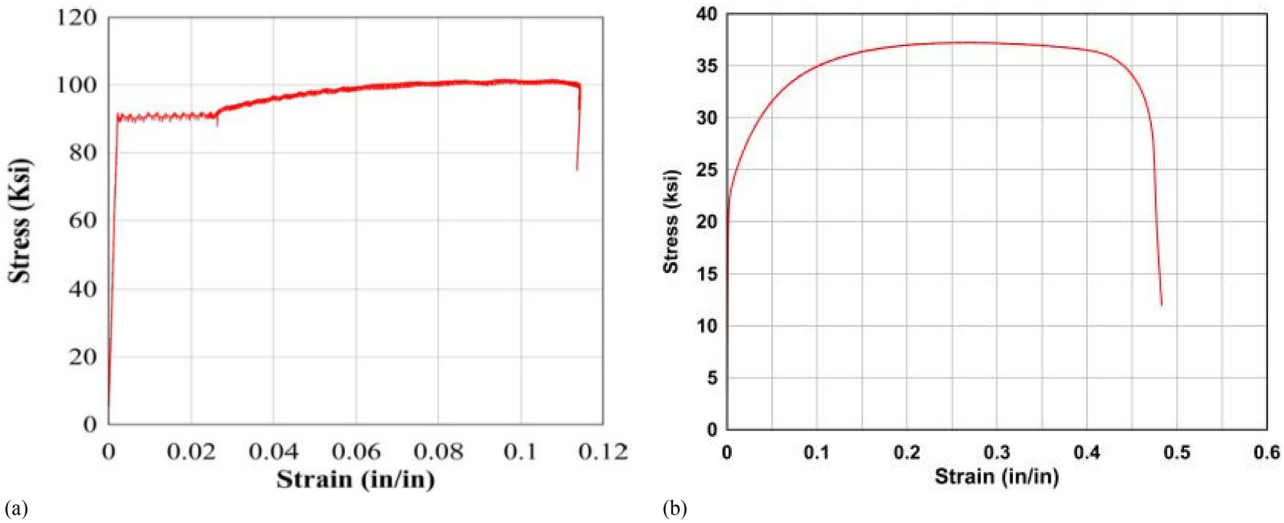

Fig. 1. Stress–strain curve for: (a) D3 wire; (b) steel jacket

(a) (b) (c)

Fig. 2. Steel collar: (a) components for column without Teflon; (b) components for column with Teflon; (c) construction (two of the four half-rings shown were installed at the base of the column, and two at the top)

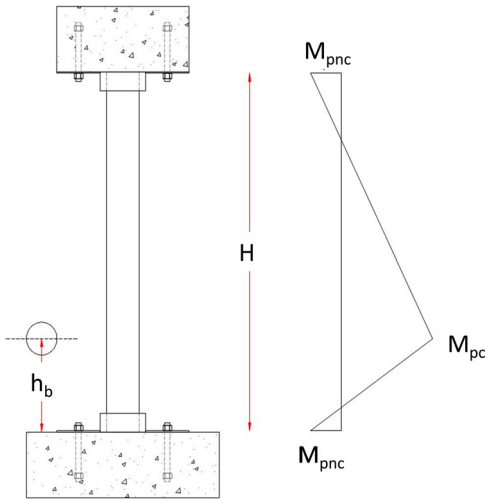

Fig. 3. Plastic moment distribution for MSJC

strength of the collar; note that the collar itself is inexpensive, as most of the retrofit cost is in the labor, so it was deemed acceptable here to use the nominal static yield strength for this calculation).

V_{pr} is the strength reached when the SJC develops its flexural capacity, calculated using the bending moment diagram shown in Fig. 3

$$V_{pr} = \frac{M_{pc} + M_{pnc}}{h_b} \tag{2}$$

where M_{pc} is the moment strength of the SJC calculated based on the assumption that the RC column and the steel jacket behave compositely for the plastic hinge located at h_b; M_{pnc} is the plastic moment of the RC column at the gap that exists at the base or at the top of a SJC; and h_b is the height of the center of the charge with respect to the base of the SJC (Fig. 3).

Furthermore, A_{c_eff} is the area of the collar effective in shear, which depends on the diameter of the collar (d_c) and its thickness (t_c), and is calculated as

$$A_{c\_\text{eff}} = 2d_c t_c \tag{3}$$

Substituting Eqs. (2) and (3) into Eq. (1) and solving for t_c leads to

$$t_c = \frac{2(M_{pc} + M_{pnc})}{2d_c h_b f_{vc}} = \frac{3(M_{pc} + M_{pnc})}{5d_c h_b F_{yc}} \tag{4}$$

The inner diameter of the collar (d_{ci}) can be used instead of d_c in Eq. (4) to obtain an estimate of its required thickness. The inner diameter of the collar is determined by allowing a gap of 0.125 in. between the SJC and the collar, such that

$$d_{ci} = D + 2 \times 0.125 \text{ in.} \tag{5}$$

where D is the diameter of the SJC.

Although the 0.125-in. gap was partly driven by construction practicalities, at any scale, the gap width only needed to be chosen to allow the development of column curvatures compatible with plastic hinging at the base of the jacketed column. Once an estimate of the thickness was obtained, it was revised accordingly to take into account the true diameter of the collar.

Because two pieces of tubes were welded together to form the collar, it was expected that, under load, the seam at the weld would be put in tension by hoop stresses. To prevent the weld from splitting, it was designed conservatively assuming that the magnitude of hoop stress (σ_θ) in the collar was

$$\sigma_\theta = \frac{V_{pr}}{t_c h_c} \tag{6}$$

In other words, the required resistance/unit length of the weld (i.e., dividing the total required strength of the weld by the weld length, L_w) was defined as

$$\frac{R_n}{L_w} = \sigma_\theta t_c = \frac{V_{pr}}{h_c} \tag{7}$$

Given that the length of the weld must be equal to the height of the collar (for practical reasons), the required unfactored resistance of the weld was therefore

$$R_n = V_{pr} \tag{8}$$

The height of the collar was determined by considering two scenarios: one in which partial contact develops at the top of the collar between the collar and the SJC, and another in which full contact between the SJC and the collar is assumed. For the deformations of the SJC and the collar to be compatible for both cases, a hinge may need to form at the base of the collar. With that assumption, the height of the collar in the first scenario, for a point load applied at the top of the collar, becomes

$$h_c = \frac{M_{cr}}{V_{pr}} \tag{9}$$

where M_{cr} is the reduced moment capacity of the collar calculated using a reduced thickness (t_{rc}) that considers the fact that part of the section is used to resist the shear V_u

$$M_{cr} = \frac{d_c^3 - (d_c - 2t_{rc})^3}{6} F_{yc} \tag{10}$$

with

$$t_{rc} = t_c \left[1 - \left(\frac{2V_{pr}}{V_{cp}} - 1 \right)^2 \right] \tag{11}$$

where V_{cp} is the theoretical plastic shear capacity of the tube calculated considering that the full cross section of the collar is effective in shear.

In the second scenario, when full contact exists between the collar and the SJC, it is assumed that shear is transferred by the SJC as a uniformly distributed load over the height of the collar, and consequently the height of the collar is equal to twice the value predicted by Eq. (9) and given by

$$h_c = \frac{2M_{cr}}{V_{pr}} \tag{12}$$

Collar heights resulting from both scenarios were considered for the tests. However, after the tests, as presented later, it was observed that full contact between the SJC and the collar was never achieved. Consequently, it was suggested that, for sizing of the collar, Eq. (9) alone be used to estimate the height.

Design of the threaded bolts used as concrete anchors at the base of the specimen was performed using Appendix D of ACI 318-11 (ACI 2011), assuming that the shear resisted by the collar was transmitted to and equally shared by the bolts. Once a tentative bolt diameter was found, the effect of the tension–shear interaction was checked according to the American Concrete Institute (ACI 2011), with the tension acting on the bolt set equal to the pretension needed to tighten it in place.

The top of a SJC may also fail in direct shear under blast load. It was therefore decided to test some MSJC specimens with a collar at their tops. The top collar was designed similarly to the bottom collar, with the only differences being that a square top plate was used, and the estimated demand at the top of the specimens was smaller than at their base (due to the greater distance between M_{pc} and M_{pnc}). Consequently, the bolts at the top of the specimen were smaller.

The final design of the retrofit called for a collar with a 229-mm (9-in.) outside diameter and a wall thickness of 4.75 mm (0.187 in.). A 9.5-mm (0.375-in.) thick base plate was found to be adequate, together with nine 19-mm (0.75-in.) diameter threaded bolts embedded 152 mm (6 in.) into the foundation. Similar dimensions were used for the top collar, except that nine 6.4-mm (0.25-in.) diameter threaded bolts were used (with a similar embedment in the cap beam). To investigate possible differences in behavior, 50.8-mm (2-in.) and 101.6-mm (4-in.) tall collars were used on different specimens.

A total of four specimens were constructed (MSJC1 to MSJC4) in accordance with the previous final design characteristics. Variations among specimens are presented in Table 1. Essentially, all specimens had 2-in. collars, except MSJC2. MSJC1, MSJC3, and MSJC4 differed only in that MSJC1 did not have a top collar, and MSJC3 did not have Rulon tape inserted between the collar and the SJC. The minimal differences among all specimens also allowed reliable comparisons of specimen behavior when subjected to blasts of varying intensity.

Table 1. MSJC Specimens

Design characteristic	Specimen			
	MSJC1	MSJC2	MSJC3	MSJC4
Collar height	50 mm (2 in.)	101.6 mm (4 in.)	50 mm (2 in.)	50 mm (2 in.)
Collar location	Bottom only	Top and bottom	Top and bottom	Top and bottom
Rulon tape	Yes	Yes	No	Yes

Instrumentation

To obtain information on the peak velocity of the specimen during its response and estimate the impulse seen, a series of shorting pins was used. The shorting pins were mounted on a Plexiglas box and positioned such that the centerline of the box assembly was aligned with the center of the explosive, 254 mm (10 in.) from the top of the foundation. When the pins were shorted during the test, the time at which contact between the pins and the specimen occurred for each individual pin was recorded using a data-acquisition system. More information on this instrumentation approach, including a figure showing the pins mounted in the Plexiglas box, the location of the pins along the specimen, and how the collected data were used, is provided in a later section.

Attempts were also made to collect acceleration histories at the back of the specimens at two different elevations (at the height of the charge and at the half-distance between that point and the top of the column) using shock accelerometers with respective capacities of 200,000g and 60,000g. However, this attempt did not yield satisfactory results because the capacities of the accelerometers were exceeded during the tests.

Strain gauges had been installed on the inside surface of the outside tube of the larger sections to collect strain histories in the regions of the specimens that were to remain elastic. Unfortunately, these gauges, installed during construction of the specimen, were not responsive when received at the test site, and consequently no data could be collected from them. Finally, overpressures were measured for all tests using a pencil pressure probe placed at a fixed standoff of 94x.

Experimental Observations on MSJCs

Specimen MSJC1

The charge weight and scaled distance (3x) used in testing MSJC1 were approximately identical to those used for Specimen SJC1 previously tested by Fujikura and Bruneau (2011) and that had failed in direct shear. Numerical values of charge weight and standoff distances are not presented here for security reasons; instead, normalized values are used, where 1.0x corresponds to a standoff distance that corresponds to a severe threat with a scaled distance of 0.12 m/kg$^{1/3}$ (0.30 ft/lb$^{1/3}$). The corresponding scaled distance is presented in Table 2, along with measured response parameters for all specimens tested (charge weight was kept constant, and only standoff distance was varied from test to test). Note that direct shear failure started to occur in the tests performed by Fujikura and Bruneau (2011) at normalized standoff distances of 3.25x.

After the test, MSJC1 deformed to a maximum of 3.18 mm (0.125 in.) at a height of 305 mm (12 in.) above the top of the foundation. No direct shear failure was observed at the base of the specimen. Some deformation was observed in the collar, but it did not affect the capacity of MSJC1 to resist the blast load. In fact, the same specimen was retested twice to push it to its limit of resistance. Upon close inspection of the specimen after those tests, a horizontal crack was found at the top of the column, suggesting initiation of a direct shear failure at that location (Figs. 4

Table 2. Blast Test Parameters and Posttest Measured Deformations of Specimens

Specimen	Normalized distance	Scaled distance [m/kg$^{1/3}$ (ft/lb$^{1/3}$)]	Maximum deformation [mm (in.)]	Base rotation (rad)	Height of maximum deformation [mm (in.)]
MSJC1	3.0x	0.12 (0.30)	3.18 (0.125)		305 (12)
MSJC1	2.57x	0.31 (0.78)	10.7 (0.42)		406 (16)
MSJC1	1.57x	0.19 (0.47)	71.6 (2.82)	0.18	406 (16)
MSJC2	1.57x	0.19 (0.47)	54 (2.13)	0.15	356 (14)
MSJC2	2.14x	0.26 (0.65)	15.2 (0.60)	0.03	457 (18)
MSJC3	1.57x	0.19 (0.47)	61 (2.40)	0.15	406 (16)
MSJC4	1.29x	0.15 (0.39)	—	—	—

(a) (b)

Fig. 4. Specimen MSJC1 after Test 1: (a) crack at top of columns; (b) deformation of collar

Fig. 5. Deformation of Specimen MSJC1 after first test

and 5). This is consistent with the observation made by Fujikura and Bruneau (2011).

A shorting pin assembly consisting of five pins was placed on the back of the specimen. Only two of these pins shorted because the deformation of MSJC1 was not enough to cause its back to touch all of the pins. Because the pins were spaced at 3.18-mm (0.125-in.) increments, with the longest one nearly touching the back of MSJC1, the specimen deformed more than the measured residual deformation, and elastic rebound occurred.

Because MSJC1 survived the first shot with minimal damage, a second test at a closer range of 2.57x was conducted on this specimen. An assembly with five shorting pins was placed on the back of MSJC1 for this retest. Measurements taken after the test showed that the specimen deformed to 10.7 mm (0.42 in.) from its initial deformation of 3.18 mm (0.125 in.). This represents roughly an 8-mm (0.315-in.) increase in deformation from the previous test. With the exception of a few notches and pits observed on the outside steel jacket, no significant deformation of the cross section of the specimen was noted. The front face of the collar deformed inward [Fig. 6(a)], likely under the action of the overpressure seen at that location. Fracture of both weld connections of the collar was noted [Fig. 6(b)]. Because the specimen was bearing on the back of the collar, hoop stress might have developed in the collar, leading to that fracture.

The crack in the concrete core that appeared at the top of MSJC1 after the first test widened [Fig. 6(d)]; however, no rebar failure was visible though the small crack, and no significant offset indicative of direct shear failure was observed. MSJC1 was therefore tested at third time.

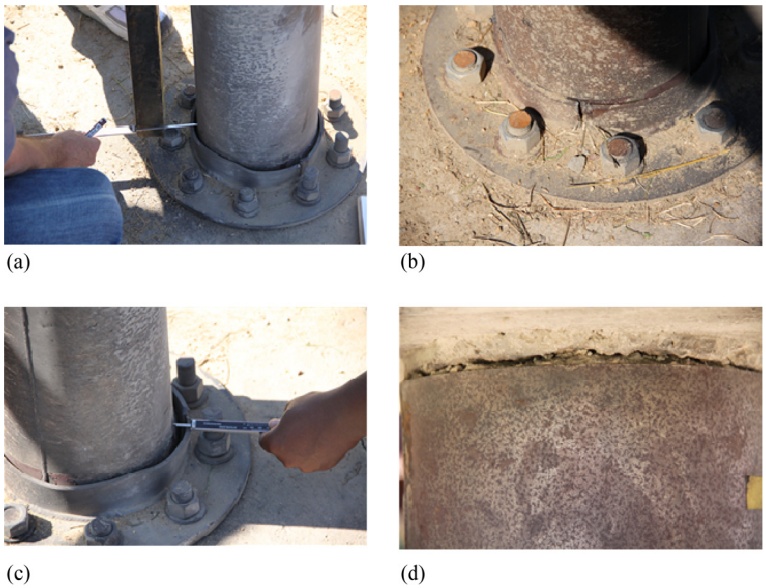

Fig. 6. Specimen MSJC1 after second test: (a) inward deformation of collar on side facing charge; (b) crack in collar at weld connection; (c) collar deformations measured using the depth probe of a vernier caliper; (d) widening of preexisting crack at top of specimen

Fig. 7. Seam failure of Specimen MSJC1 and base deformation

The damage to the collar of MSJC1 from its previous tests was repaired before this third test. The lip of the tear was reinforced with a 0.25-in. thick piece of steel and welded. The scaled distance between the charge and the target was set at $1.57x$. An assembly of ten shorting pins was placed on the back of the specimen.

After the test, several additional buckling waves on the front face of MSJC1 and failure of the vertical weld seam were visible (Fig. 7). The repaired collar did not suffer any damage. During its deformation, the steel jacket came into contact with the collar, leaving a visible horizontal indentation at that location (Fig. 8). The additional deformation demand on the specimen from this test caused the steel jacket to slip over the internal face of the collar on the side exposed to the blast. The back of the collar rotated and deformed but did not fail. The lip of the base plate exposed to the blast deformed upward, causing some of the threaded rod in front of the blast to rotate (Fig. 9).

The overall mechanism of deformation at the base of the specimen possibly occurred in the following sequence (Fig. 10). First, the front of the collar came into contact with the steel jacket as the specimen deformed [Fig. 10(a)], but the local contact forces on the front did not prevent slipping between the collar and the jacket. In the meantime, on the back, the deforming specimen bore against the back of the collar, pushed it out, and caused it to deform [Fig. 10(b)]. Contact was followed by slippage on the front, as evidenced by the tearing of the Rulon tape [Figs. 10(c) and 11], whereas on the back, after bearing against the collar, a clear deformation mark was left on the steel jacket. The behavior is believed to

have been similar for all specimens, with respective differences described in the following subsections.

The crack visible at the top of the specimen from the first test widened further, exposing the reinforcement of the column. On inspection, none of the rebars were severed. From approximately 12.7-mm (0.5-in.) deformation from the two previous tests, MSJC1 deformed an additional 61 mm (2.40 in.). This deformation was measured at a height of 406 mm (16 in.); this corresponds to 0.15 rad of additional base rotation. The final rotation at the end of the test was 0.18 rad.

Fig. 8. Mark on steel jacket resulting from bearing on collar

Specimen MSJC2

MSJC2 had 4-in. collars top and bottom (Fig. 12) and was tested only once. The length of the longer collar was established assuming that load transmitted from the specimen to the collar would result in the latter failing in flexure while following the rotation at the base of the specimen. The scaled distance of $1.57x$ was chosen such that direct comparisons could be made with MSJC1 and MSJC3, which were also tested at the same scaled distance and had 2-in. collars.

To enhance the resolution with which the velocity history at the back of the specimen was captured, the number of shorting pins in the assembly was increased to 10. The pins were divided between two blocks of five pins. All of the pins were shorted at the end of the test.

Postblast measurements on MSJC2 showed that the specimen deformed up to 54 mm (2.13 in.) at a height of 356 mm (14 in.).

Fig. 9. Damage to Rulon tape and slip of Specimen MSJC1 over collar

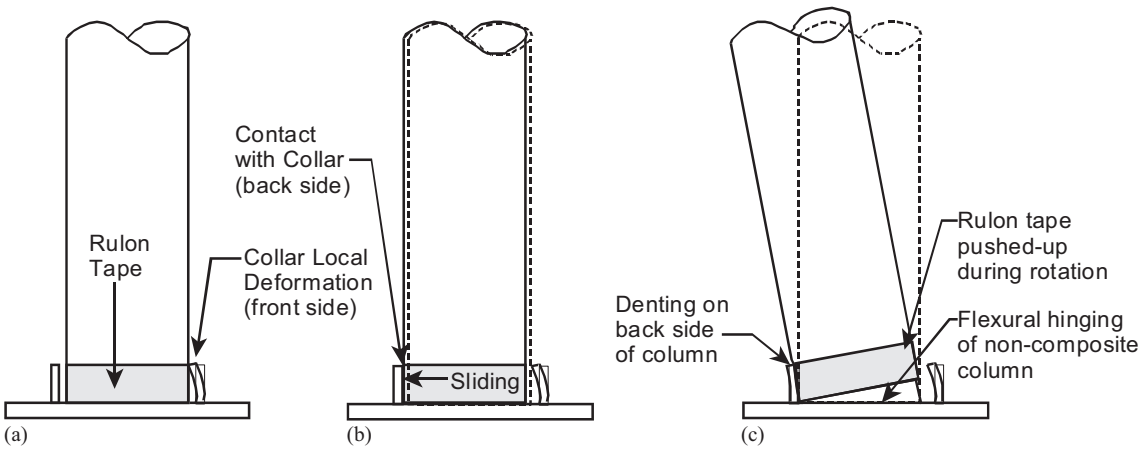

Fig. 10. Mechanism of deformation at base of specimen

This corresponds approximately to 0.15 rad of rotation at the base of the specimen. Splitting and opening of the collar in the back of the specimen were observed as a consequence of this important rotation demand (Fig. 13). Several buckling lobes (Fig. 14) developed on the front face of the specimen. The jacketed column and the collar came into contact near the top, as evidenced by a mark on the steel jacket matching the location of the collar.

Specimen MSJC3

MSJC3 was identical to MSJC4 except that MSJC3 did not have Rulon tape at the interface between the steel jacket and the collar. MSJC3 was first tested at a scaled distance of 2.14x. The shorting pin assembly for this test consisted of five pins. Only four of the five pins were deformed after the test.

Deformation of the collar at the front and back of the specimen was noted. A tear at the junction of the two halves of the collar at the base was also observed, again possibly due to hoop stress in the collar exceeding the capacity of the weld. The lip of the base plate of this collar deformed upward, possibly due to blast overpressure entering a small gap existing between the plate and the top of the foundation. However, the top collar did not suffer any visible damage.

Fig. 11. Widening of crack at top of Specimen MSJC1

MSJC3 did not deform much under load. The maximum permanent deformation over the height of the specimen was 15.3 mm (0.60 in.) at a height of 457 mm (18 in., 0.03 rad). Measurement of the diameters of the specimen at the height of the blast charge showed that some marginal deformation in cross section occurred, but there was no significant ovalization of the section.

After repairing the collar of MSJC3 to restore its resistance, the specimen was retested. Some of the front nuts of the base plate were found to be slightly loose after the prior tests because the lip of the base plate had deformed upward. Therefore, the nuts were retightened prior to the second test. The shorting pin arrangement on the back of MSJC3 consisted of 10 pins mounted on two blocks. The scaled distance was set at 1.57x.

The final maximum deformation of MSJC3 was identical to that of MSJC1 [61 mm (2.40 in.) at a height of 406 mm (16 in.) or 0.18 rad at the base]. The additional deformation from the first to the second test in that case was 45.7 mm (1.80 in.). Several buckling waves developed in the front face of MSJC3 (Fig. 15). Contrary to observations on MSJC1, the seam of MSJC3 survived the test. For comparison, note that MSJC3 was tested twice (at scaled distances of 2.14x and 1.57x) and that MSJC1 was tested three times (at scaled distances of 3.00x, 2.57x, and 1.57x).

Plastic deformations (Fig. 16) in the bottom collar did not cause failure at the weld connection, as observed in the first test. Slippage between the collar and the steel jacket was observed in mostly the same fashion as in the last test on MSJC1 [Fig. 16(a)]. The top collar remained undamaged and virtually undeformed (Fig. 17).

Specimen MSJC4

MSJC4 was similar to MSJC1 except that, because direct shear failure was anticipated at the top of the specimen and to prevent such failure, a collar was also provided at that location in addition to the one used at the bottom. The scaled distance for the specimen was

Fig. 12. View of collars of Specimen MSJC2

Fig. 13. Postshot failure of collar on Specimen MSJC2

Fig. 14. Specimen MSJC2 after test

Fig. 15. Deformation of Specimen MSJC3 after second test

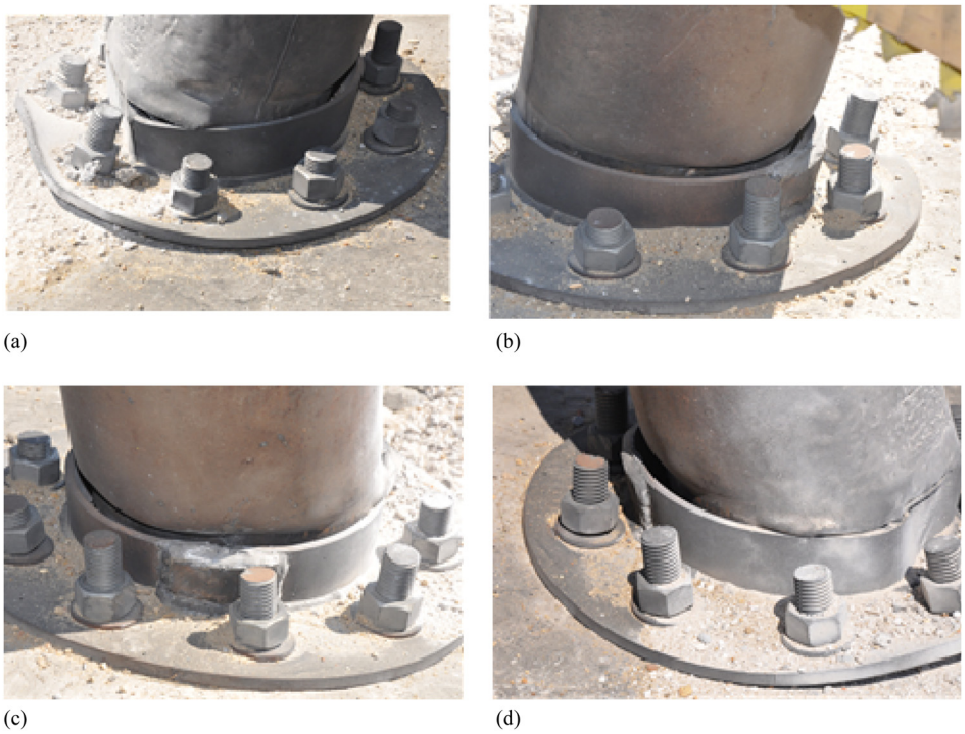

Fig. 16. State of bottom collar after second test of Specimen MSJC3

Fig. 17. State of top collar after second test of MSJC3

reduced to $1.29x$ for this test, i.e., the smallest value considered in all tests. No shorting pins were used in this test.

During the blast, the steel jacket was torn along its seam (Fig. 18). As a consequence, the concrete column became exposed, and several rebars and spiral reinforcements fractured near the base of the specimen. The observed unzipping of the seam was attributed to failure of its weld. Because the confinement provided by the steel jacket was lost and the RC column inside the jacket was not ductile, the column lost its capacity to carry load. As the weakest point of pipes/tubes used in structural engineering application is typically not the vertical seam weld, this failure possibly occurred as a consequence of fabrication errors due to the small scale considered here.

Notable deformations and failure at the weld connections of the collar were observed in both the front and back of the column (Fig. 18). This led to the conclusion that the front rim of the collar was subjected to significant overpressures, whereas excessive deformation of the specimen generated important hoop stresses in the back ring.

Characterization of Blast Loading Applied to MSJCs Using Shorting Pins

Methodology

As mentioned previously, shorting pins were mounted on a Plexiglas box and positioned such that the assemblages of shorting pins had their center of gravity located at the same height as the center of the detonated charge (i.e., 10 in. from the top of the foundation). These were placed on the back face of a few specimens. As a specimen deformed under blast overpressure, the pins touched the specimen, and the current in the pin was short-circuited (i.e., the pins were shorted). The number of pins that were shorted depended on the magnitude of the deformation and, hence, on the impulse imparted to the specimen. As the pins were shorted, the time at which the back face of the specimen contacted the extremity of each pin was recorded. The distance between the back face of the specimen and the extremities of the multiple pins used were preset.

Fig. 18. Global view and close-up of base of Specimen MSJC4 after test

Based on the spacings and times of arrival of the back face of the specimen at the pin tips, a portion of the velocity history of the back face of the specimen could then be determined. An estimate of the resultant impulse at the height of burst could be established based on the velocity history on the back face of a specimen. This approach is valid provided that the cross section of the specimen maintains its shape (as was the case here). For a deforming cross section, each point of the cross section will be moving at a specific velocity, and the estimate of the impulse will be somewhat affected.

If the spacing between the extremities of Pins 1 to n and the back face of the specimen at rest are designated by $x_1, x_2, ..., x_i, ..., x_n$, respectively, and the corresponding times at which contact with the pins occurs are $\tau_1, \tau_2, ..., \tau_i, ..., \tau_n$, then the velocities, v_i, at which the back face of the specimen travels from the extremity of Pin i to that of Pin $i + 1$ can be obtained using

$$v_i = \frac{x_{i+1} - x_i}{\tau_{i+1} - \tau_i}, \ 1 \leq i \leq n \tag{13}$$

where n is the number of pins. The velocity history at the back face of the specimen is given by the pair (τ_i, v_i). If it is assumed that the velocity history so calculated represents the velocity of the back of the specimen at the same height as the center of the charge (which is where the pins are located), the resultant impulse/unit length seen by that section can be estimated as the product of the mass of the section (mass/unit length of the specimen) and the velocity so calculated. The impulse/unit area, i_i, normally reported by software such as *BEL 1.1.0.3* is obtained by dividing the impulse/unit length, I_i, by the breadth or the diameter (D) of the section exposed to the blast

$$I_i = mv_i, \ 1 \leq i \leq n \tag{14}$$

$$i_i = \frac{I_i}{D}, \ 1 \leq i \leq n \tag{15}$$

Application to Test Series

It was found that, with less than 10 pins, the velocity history at the back of a specimen was too severely truncated, and no estimate of the peak or the deceleration of the specimen afterwards could be obtained for those cases. For specimens instrumented with 10 pins, Fig. 19 illustrates a typical pin assemblage on the back face of the element. The 10 pins were split between two blocks (Blocks A and B) of five pins each, allowing the calculation of 10 data points of the velocity history on the back face of the specimen. The distances between the tip of each pin and the back face of the specimen were calculated, and the times of contact between the back face of the specimen and each pin were obtained from the data collected for the pins. The times of arrival for all specimens instrumented with the 10-pin assemblies are reported in Table 3, along with the velocities and impulses calculated per the equations from the previous section.

Summary and Conclusions

A MSJC concept has been proposed. This retrofit detail was designed to add blast resistance to bridge columns seismically

Fig. 19. Shorting pin assembly on back of MSJC2 (Block A is hidden behind Block B)

Table 3. Velocity and Impulse for MSJC Specimens

Specimen	x_i (mm)	τ_i (s)	v_i (s)	I_i (MPa/ms)
MSJC1	1.83	2.95×10^{-4}	6.21	2.24
	4.76	3.98×10^{-4}	28.5	10.25
	5.86	4.04×10^{-4}	183	66.00
	8.43	4.49×10^{-4}	5.7	20.53
	12.09	5.67×10^{-4}	31	11.19
	17.22	6.52×10^{-4}	60.3	21.74
	17.95	8.44×10^{-4}	3.82	1.38
	18.68	8.68×10^{-4}	30.5	11.00
	26.74	9.65×10^{-4}	83.1	29.94
MSJC2	4.32	2.22×10^{-4}	19.4	7.00
	8.38	3.28×10^{-4}	38.6	13.92
	12.19	3.36×10^{-4}	448	161.52
	16.76	4.29×10^{-4}	49.2	17.71
	23.88	5.35×10^{-4}	67.1	24.18
	28.96	6.15×10^{-4}	63.5	22.88
	36.07	7.23×10^{-4}	65.9	23.73
	42.42	8.56×10^{-4}	47.7	17.20
	48.77	9.68×10^{-4}	56.7	20.43
MSJC3	2.16	2.68×10^{-4}	8.08	2.91
	5.20	3.59×10^{-4}	33.3	12.00
	8.23	3.91×10^{-4}	94.7	34.13
	10.39	4.58×10^{-4}	32.3	11.64
	14.29	5.95×10^{-4}	28.4	10.25
	17.75	6.11×10^{-4}	216	78.00
	21.65	7.99×10^{-4}	20.7	7.47
	22.08	8.12×10^{-4}	33.3	12.00
	28.58	1.11×10^{-4}	22.2	7.99

retrofitted using steel jackets because the seismically retrofitted detail alone is known to be vulnerable to direct shear failure.

The modification to the SJCs consisted of adding, at the bottom and top of the column, structural steel collars designed to transfer (by contact) the column shears to the footing and bent cap. Blast tests conducted to investigate the effectiveness of this simple proposed detail demonstrated its effectiveness in preventing direct shear failure. Severe blast load demands were applied to investigate the behavior of the retrofitted column under extreme ductility demands. Except for one specimen that uncharacteristically failed due to fracture of the tube's vertical weld seam, all specimens exhibited satisfactory ductile behavior, with maximum base rotations of up to 0.15–0.18 rad. For comparison, note that AISC 341 (AISC 2010) considers beam-to-column connections that can cyclically develop 0.04 rad to be highly ductile and that UFC 3-340-02 (DoD 2008) qualifies rotations of 2–5° (0.035–0.09 rad) as moderate damage and 5–12° (0.09–0.21 rad) as severe damage.

Future Research

In the specimens tested here, the flexible collars that converted SJCs into MSJCs were relatively flexible, and there is no reason to believe that their addition would degrade the ability of the columns to develop their ductile noncomposite flexural response within the collars. However, this may not remain the case for stiffer rings. Future research is desirable to analytically and experimentally determine the possible conditions for which the collars could detrimentally affect seismic performance. Furthermore, full-scale testing would also be helpful to verify and validate the findings reported in this study.

Acknowledgments

This research was partly supported by the Federal Highway Administration under an award to the Multidisciplinary Center for Earthquake Engineering Research and by the Infrastructure Protection and Disaster Management Division, Science and Technology Directorate, U.S. Department of Homeland Security, under a cooperative agreement with the Engineer Research Development Center of the U.S. Army Corps of Engineers (Contract W912HZ-11-2-0001). Any opinions, findings, conclusions, and recommendations presented in this paper are those of the authors and do not necessarily reflect the views of the sponsors. Permission to publish was granted by the Director, Geotechnical and Structures Laboratory.

References

ACI (American Concrete Institute). (2011). "Building code requirements for structural concrete and commentary." *ACI 318-11*, Farmington Hills, MI.

AISC. (2010). "Seismic provisions for structural steel buildings." *AISC 341-10*, Chicago.

ASTM. (2015). *ASTM 1008 CS*, West Conshohocken, PA.

BEL [Computer software]. U.S. Army Engineer Research and Development Center, Vicksburg, MS.
Buckle, I. G., Friedland, I., Mander, J., Martin, G., Nutt, R., and Power, M. (2006). "Seismic retrofitting manual for highway structures: Part 1—Bridges." *Technical Rep. MCEER-06-SP10*, Univ. at Buffalo, Buffalo, NY.
Caltrans. (1996). *Earthquake retrofit guidelines for bridges, memo to designers 20-4*, Sacramento, CA.
Chai, Y. H. (1996). "An analysis of the seismic characteristics of steel-jacketed circular bridge columns". *Earthquake Eng. Struct. Dyn.*, 25(2), 149–161.
Chai, Y. H., Priestley, M. J. N., and Seible, F. (1991). "Seismic retrofit of circular bridge columns for enhanced flexural performance." *ACI Struct. J.*, 88(5), 572–584.
DoD (Department of Defense). (2008). "Structures to resist the effects of accidental explosions." *Rep. UFC 3-340-02*, Arlington, VA.
Fouché, P., and Bruneau, M. (2014). "Blast and seismic resistant concrete-filled double skin tubes and modified steel jacketed bridge columns." *Techinical Rep. MCEER-14-004*, Univ. at Buffalo, Buffalo, NY.
Fujikura, S., and Bruneau, M. (2011). "Experimental investigation of seismically resistant bridge piers under blast loading." *J. Bridge Eng.*, 10.1061/(ASCE)BE.1943-5592.0000124, 63–71.
Fujikura, S., and Bruneau, M. (2012). "Dynamic analysis of multihazard-resistant bridge piers having concrete-filled steel tube under blast loading." *J. Bridge Eng.*, 10.1061/(ASCE)BE.1943-5592.0000270, 249–258.
Fujikura, S., Bruneau M., and Lopez-Garcia, D. (2008). "Experimental investigation of multihazard resistant bridge piers having concrete-filled steel tube under blast loading." *J. Bridge Eng.*, 10.1061/(ASCE)1084-0702(2008)13:6(586), 586–594.
Housner, G. W., and Thiel, C. C. (1990). "Competing against time: Report of the Governor's Board of Inquiry on the 1989 Loma Prieta Earthquake." *Earthquake Spectra*, 6(4), 681–711.
Kim, S. H., and Shinozuka, M. (2004). "Development of fragility curves of bridges retrofitted by column jacketing. *Probab. Eng. Mech.*, 19(1), 105–112.
Priestley, M. J. N., Seible, F., and Calvi, G. M. (1996). *Seismic design and retrofit of bridges*, John Wiley & Sons, New York.
Priestley, M. J. N., Seible, F., Xiao, Y., and Verma, R. (1994). "Steel jacket retrofitting of reinforced concrete bridge columns for enhanced shear strength—Part 1: Theoretical considerations and test design." *ACI Struct. J.*, 91(4), 394–405.
Shams, M., and Saadeghvaziri, M. A. (1997). "State of the art of concrete-filled steel tubular columns." *ACI Struct. J.*, 94(5), 558–571.
Williams, D., Holland, C., Williamson, E., Bayrak, O., Marchand, K., and Ray, J. (2008). "Blast-resistant highway bridges: Design and detailing guidelines." *Proc., 10th Int. Conf. on Structures under Shock and Impact (SUSI)*, WIT Press, Southampton, U.K.
Woodson, S. C., and Baylot, J. T. (1999). "Structural collapse: Quarter-scale model experiments." *Technical Rep. SL-99-8*, U.S. Army Engineer Research and Development Center, Vicksburg, MS.